doi:10.1111/j.1558-5646.2010.01025.x

EARLY BURSTS OF BODY SIZE AND SHAPE EVOLUTION ARE RARE IN COMPARATIVE DATA

Luke J. Harmon,[1,2,3] Jonathan B. Losos,[4] T. Jonathan Davies,[5] Rosemary G. Gillespie,[6] John L. Gittleman,[7] W. Bryan Jennings,[8] Kenneth H. Kozak,[9] Mark A. McPeek,[10] Franck Moreno-Roark,[11] Thomas J. Near,[12] Andy Purvis,[13] Robert E. Ricklefs,[14] Dolph Schluter,[2] James A. Schulte II,[11] Ole Seehausen,[15,16] Brian L. Sidlauskas,[17,18] Omar Torres-Carvajal,[19] Jason T. Weir,[2] and Arne Ø. Mooers[20]

[1]Department of Biological Sciences, University of Idaho, Moscow, Idaho 83844

[2]Biodiversity Centre, University of British Columbia, Vancouver, BC V6T1Z4, Canada

[3]E-mail: lukeh@uidaho.edu

[4]Department of Organismic and Evolutionary Biology, Harvard University, Cambridge, Massachusetts 02138

[5]National Center for Ecological Analysis and Synthesis, University of California, Santa Barbara, 735 State Street, Suite 300, Santa Barbara, California 93101

[6]Department of Environmental Science, Policy and Management, University of California, Berkeley, California 94720

[7]Odum School of Ecology, University of Georgia, Athens, Georgia 30602

[8]Department of Biological Sciences, Humboldt State University, Arcata, California 95521

[9]Department of Fisheries, Wildlife, and Conservation Biology, University of Minnesota, St. Paul, Minnesota 55108

[10]Department of Biological Sciences, Dartmouth College, Hanover, New Hampshire 03755

[11]Department of Biology, Clarkson University, Potsdam, New York 13699

[12]Department of Ecology and Evolutionary Biology, Yale University, New Haven, Connecticut 06520

[13]Division of Biology, Imperial College London, Silwood Park Campus, Ascot, SL5 7PY United Kingdom

[14]Department of Biology, University of Missouri—St. Louis, St. Louis, Missouri 63121

[15]Institute of Ecology & Evolution, Division of Aquatic Ecology & Macroevolution, University of Bern, CH-3012 Bern, Switzerland

[16]Eawag Centre of Ecology, Evolution and Biogeochemistry, Department of Fish Ecology & Evolution, Seestrasse 79, CH-6047 Kastanienbaum, Switzerland

[17]National Evolutionary Synthesis Center, Durham, North Carolina 27705

[18]Oregon State University, Department of Fisheries and Wildlife, 104 Nash Hall, Corvallis, Oregon, 97331

[19]Escuela de Biología, Pontificia Universidad Católica del Ecuador, Apartado 17-01-2184, Quito, Ecuador

[20]Department of Biological Sciences, Simon Fraser University, Burnaby, BC V5A1S6, Canada

Received May 11, 2009
Accepted February 21, 2010

George Gaylord Simpson famously postulated that much of life's diversity originated as adaptive radiations—more or less simultaneous divergences of numerous lines from a single ancestral adaptive type. However, identifying adaptive radiations has proven difficult due to a lack of broad-scale comparative datasets. Here, we use phylogenetic comparative data on body size and shape in a diversity of animal clades to test a key model of adaptive radiation, in which initially rapid morphological evolution is followed by relative stasis. We compared the fit of this model to both single selective peak and random walk models. We found little support for the early-burst model of adaptive radiation, whereas both other models, particularly that of selective peaks, were commonly supported. In addition, we found that the net rate of morphological evolution varied inversely with clade age. The youngest clades appear to evolve most rapidly because long-term change typically does not attain the amount of divergence predicted from rates measured over short time scales. Across our entire analysis, the dominant pattern was one of constraints shaping evolution continually through time rather than rapid evolution followed by stasis. We suggest that the classical model of adaptive radiation, where morphological evolution is initially rapid and slows through time, may be rare in comparative data.

KEY WORDS: Adaptive radiation, Brownian motion, comparative methods, model fitting, phylogeny.

Although the concept of adaptive radiation traces back to Henry Fairfield Osborn (1902), it was George Gaylord Simpson (1944, 1953) who brought the idea to the forefront of evolutionary biology. Simpson defined adaptive radiation as "more or less simultaneous divergences of numerous lines from more or less the same ancestral adaptive type" (Simpson 1959), and famously postulated that much of life's diversity originated during these adaptive radiations. However, identifying adaptive radiations has proven difficult due to a lack of broad-scale comparative datasets. In fact, almost all accepted adaptive radiations come from endemic radiations of species on isolated oceanic islands or lakes (e.g., Baldwin and Sanderson 1998; Givnish 1999; Gillespie 2004; Grant and Grant 2008; Losos 2009). Beyond these systems, criteria for recognizing adaptive radiations are murky (but see Givnish 1997; Schluter 2000), and their prevalence in the tree of life uncertain.

Several theories predict how adaptive radiation might proceed (see Schluter 2000). Some of these focus on lineage accumulation (e.g., see many chapters in Givnish and Sytsma 1997). Recent analyses indicate a prevalence of early rapid accumulation of lineages followed by a slowdown in net diversification through time (Nee et al. 1992; Seehausen 2006; McPeek 2008; Phillimore and Price 2008; Rabosky and Lovette 2008; Linder 2009). We focus here on the tempo and mode of morphological evolution, which is more closely related to Simpson's (1944) model in which organisms diversify upon entering new adaptive zones (Losos and Miles 2002). Simpson's adaptive zones represent sets of similar niches that are ecologically available to a particular lineage and free from potential competitors. When lineages first enter these zones, morphological evolution should initially be rapid; as ecological space becomes filled, the rate of morphological evolution should then slow (Simpson 1944; Foote 1994; Schluter 2000; Blomberg et al. 2003). We refer to this as the "early burst" (EB) model, and return to the relationship between the tempo of lineage diversification and that of morphological evolution in the discussion.

We applied a phylogenetic comparative approach to test Simpson's model and investigate the dynamics of phenotypic evolution across the history of clades. Most previous studies of evolutionary rates have used comparisons of characters at the beginning and end of a given time interval (Gingerich 1983, 2001; Hendry and Kinnison 1999; Kinnison and Hendry 2001; Estes and Arnold 2007). Recent advances in phylogenetic comparative methods have opened new approaches to reconstructing the temporal dynamics of evolution when time series are not available (Martins 1994; Harmon et al. 2003; Butler and King 2004; O'Meara et al. 2006). These methods rely on two types of information: the distribution of phenotypes of contemporaneous species in a given group, and the historical relationships of species summarized in a phylogenetic tree. We develop this approach further here. The goal of our study was to test a particular pattern of adaptive radiation, the EB model in which evolution is fastest early in a clade's history and slows through time, across a large comparative dataset.

Methods

We obtained dated phylogenies and body size and shape measurements for 49 clades of animals. The clades spanned a wide range of species richness and each corresponded to an easily recognizable taxon (e.g., Felidae), many of which were geographically localized (e.g., Galápagos finches). Our dataset included several examples of clades commonly recognized as adaptive radiations, including Hawaiian *Tetragnatha* spiders, Galapagos finches, *Anolis* lizards, and African lake cichlids. Details of sample size, clade age, method of phylogenetic tree construction, and body size data are summarized in Table 1. This table also provides the estimated generation time of individuals within each clade, calculated as the average age to maturity among all species for which data were available. We created larger trees for some analyses by combining individual trees within major taxonomic groups, grafting the

Table 1. Details of sample size, clade age, method of phylogenetic tree construction, and body size data. This table also provides the estimated generation time for each clade, calculated as the average age to maturity among all species for which data were available. We also list the maximum likelihood estimate of the net rate of body size evolution (σ^2) see Supporting Information Appendix Tables 2 and 3 for other parameter estimates. The rate of evolution for one clade (*Vermivora*) could not be estimated because differences among species are smaller than the expected variation due to measurement error alone; this dataset was excluded from further analyses. We also list the Akaike weights for the BM, SSP, and EB models for body size and shape for all clades with at least 10 species. Bold indicates the model with the highest AIC weight.

Group	Clade	*n*	*n* in tree	Clade age (million years)	Tree building method	Gen. time (months)	Size variable	Rate of body size evolution	Body size AIC weights			Body shape AIC weights		
									BM	SSP	EB	BM	SSP	EB
Squamates	1. Agamidae	381	179	118[‡]	ML+PL[Δ]	9.3	SVL[Δ]	0.53	0.25	**0.66**	0.09	0	**1**	0
	2. *Anolis* (Carib.)	150	73	40[1]	ML+PL[2]	7.3	SVL[3]	0.73	**0.58**	0.2	0.22	0.04	**0.94**	0.01
	3. Corytophaninae	9	9	65[‡]	ML+PL[Δ]	16	SVL[Δ]	0.10						
	4. Chamaeleonidae	161	29	94[‡]	ML+PL[4]	5	SVL[Δ]	0.69	0.40	**0.49**	0.11	0	**1**	0
	5. Iguaninae	36	9	65[‡]	ML+PL[Δ]	58.4	SVL[Δ]	0.43						
	6. Liolaemini	204	67	74[‡]	ML+PL[Δ]	24	SVL[Δ]	0.41	0.02	**0.97**	0.01	0	**1**	0
	7. *Phelsuma*	44	20	6.0[5,6]	ML+PL[5]	6	SVL[5]	2.72	0.33	**0.59**	0.08	**0.65**	0.19	0.16
	8. Phrynosomatinae	125	70	75[‡]	ML+PL[Δ]	12.6	SVL[Δ]	0.31	**0.51**	0.32	0.17	**0.59**	0.20	0.21
	9. Pygopodidae	38	31	37[‡]	ML clock[7]	60	SVL[7]	0.42	**0.58**	0.17	0.26	0.31	0.09	**0.61**
	10. *Stenocercus*	61	29	41[‡]	ML+PL[8]	12	SVL[Δ]	0.09	**0.45**	0.43	0.13	0.43	**0.46**	0.12
	11. *Varanus*	62	38	112[‡]	ML+PL[9]	37.8	SVL[10]	0.30	0.29	0.09	**0.63**	**0.45**	0.41	0.14
Birds	12. Alcidae	24	19	10[‡]	Bayes+PL[Δ]	63	TarL[Δ†]	1.08	**0.67**	0.16	0.17	**0.67**	0.16	0.17
	13. Icteridae 1 ◊ (North American)	19	10	7.7[‡]	Bayes+PL[Δ]	18	TarL[Δ†]	1.82	**0.84**	0.08	0.08	**0.84**	0.08	0.08
	14. Icteridae 2 § (South American)	18	15	8.5[‡]	Bayes+PL[Δ]	18	MandL[Δ]	0.82	**0.72**	0.14	0.14	**0.61**	0.27	0.12
	15. *Catharus*	13	11	8.0[‡]	Bayes+PL[Δ]	12	TarL[Δ†]	0.17	**0.75**	0.17	0.09	0.29	**0.67**	0.03
	16. *Chlorospingus*	18	16	8.4[‡]	Bayes+PL[Δ]	12	TarL[Δ]	0.14	0.16	**0.81**	0.03	0.00	**1.00**	0.00
	17. *Empidonax*	15	14	8.1[‡]	Bayes+PL[Δ]	18	TarL[Δ†]	0.14	0.22	**0.74**	0.04	0.09	**0.89**	0.02
	18. Geospizini	15	14	2.5[11]	UPGMA[11]	12	TarL[12,13]	1.74	**0.58**	0.32	0.10	**0.74**	0.13	0.13
	19. Gruinae	13	13	15.0[‡]	Bayes+PL[14]	48.2	$\sqrt[3]{Mass}$[14]	0.23	**0.59**	0.31	0.10			
	20. *Icterus*	27	23	7.3[‡]	Bayes+PL[Δ]	12	TarL[Δ†]	0.20	**0.66**	0.17	0.17	**0.59**	0.26	0.15
	21. *Muscisaxicola*	12	12	8.0[‡]	Bayes+PL[Δ]	18	MandL[Δ]	2.71	0.22	**0.75**	0.03	0.14	**0.84**	0.02
	22. *Passerina*	7	6	5.5[‡]	Bayes+PL[Δ]	19.6	TarL[Δ†]	0.25						
	23. *Piranga*	10	10	10.8[‡]	Bayes+PL[Δ]	12	TarL[Δ†]	0.09	**0.73**	0.21	0.07	**0.84**	0.08	0.09
	24. *Poecile*	7	6	4.8[‡]	Bayes+PL[Δ]	12	TarL[Δ†]	0.30						
	25. *Psarocolius*, *Clypicterus*, *Ocyalus*, and *Cacicus*	20	16	8.9[‡]	Bayes+PL[Δ]	24	TarL[Δ†]	0.74	**0.70**	0.14	0.16	**0.70**	0.16	0.14

Continued.

Table 1. Continued.

Group	Clade	*n*	*n* in tree	Clade age (million years)	Tree building method	Gen. time (months)	Size variable	Rate of body size evolution	Body size AIC weights			Body shape AIC weights		
									BM	SSP	EB	BM	SSP	EB
	26. Ptilonorhynchidae	20	11	14.5‡	Bayes+PL$^{\Delta}$	45	TarL$^{\Delta\dagger}$	0.19	**0.79**	0.09	0.11	**0.78**	0.13	0.09
	27. *Ramphocelus*	8	6	6.0‡	Bayes+PL$^{\Delta}$	12	TarL$^{\Delta\dagger}$	0.20						
	28. *Sylvia*	22	17	12.0‡	Bayes+PL$^{\Delta}$	12	TarL$^{\Delta\dagger}$	0.08	**0.70**	0.15	0.15	**0.57**	0.31	0.12
	29. *Tachycineta*	8	7	7.3‡	Bayes+PL$^{\Delta}$	12	TarL$^{\Delta\dagger}$	0.08						
	30. *Toxostoma*	10	6	5.9‡	Bayes+PL$^{\Delta}$	12	TarL$^{\Delta\dagger}$	0.13						
	31. *Vermivora*	7	6	5.0‡	Bayes+PL$^{\Delta}$	12	TarL$^{\Delta\dagger}$	0.00						
	32. *Xiphorhynchus*	17	15	8.2‡	Bayes+PL$^{\Delta}$	18	TarL$^{\Delta\dagger}$	0.07	**0.58**	0.11	0.30	0.01	**0.99**	0
Fish	33. Centrarchidae	20	20	24.8[15–17]	Bayes+PL[15–17]	36	SL[15–17]	0.87	0.00	**1.00**	0.00	**0.64**	0.20	0.15
	34. Cichlids (Lake Makgadikgadi)	22	17	0.45[18]	ML+clock[18]	9	SL[18]	211.2	0.00	**1.00**	0.00	0.01	**0.99**	0.00
	35. Cichlids (South African Rivers)	6	6	3.8[18]	ML+clock[18]	9	SL[18]	2.56						
	36. Cichlids (East African Rivers)	10	7	3.2[18]	ML+clock[18]	9	SL[18]	5.82						
	37. Cichlids (Lake Tanganyika)	162	76	16‡	ML+clock$^{\Delta}$	9	SL$^{\Delta}$	3.16	0	**1.00**	0			
	38. Etheostomatinae	200	122	30.8[19–21]	Bayes+PL[19–21]	18	SL[19–21]	0.72	0	**0.99**	0	0.38	**0.48**	0.13
Arthropods	39. *Enallagma*	42	12	10[22]	ML+clock[22]	12	$\sqrt[3]{Mass}$**[22]	0.51	0.03	**0.96**	0			
	40. *Lestes*	16	7	7[22]	ML+clock[23]	12	$\sqrt[3]{Mass}$**[22]	0.55						
	41. *Tetragnatha*	62	62	5[24,25]	UPGMA[24,25]	8	TL[24,25]	6.99	**0.47**	0.37	0.16	**0.60**	0.20	0.20
Mammals	42. Canidae	34	33	5.5[26]	Supertree[26]	14.5	$\sqrt[3]{Mass}^{\Delta}$	2.62	**0.58**	0.25	0.17	0	**1**	0
	43. Felidae	36	36	13.9[26]	Supertree[26]	24.4	$\sqrt[3]{Mass}^{\Delta}$	2.21	**0.60**	0.18	0.23	0.01	**0.99**	0
	44. Mustelidae	65	62	19.9[26]	Supertree[26]	16.1	$\sqrt[3]{Mass}^{\Delta}$	1.54	**0.60**	0.20	0.21			
	45. Herpestidae	37	31	17.4[26]	Supertree[26]	15.2	$\sqrt[3]{Mass}^{\Delta}$	0.64	**0.61**	0.21	0.18			
	46. Primates (Old World)	97	89	32.4[27]	Supertree[27]	59	$\sqrt[3]{Mass}^{\Delta}$	0.51	**0.59**	0.20	0.20			
	47. Strepsirrhini	47	44	52[27]	Supertree[27]	19.2	$\sqrt[3]{Mass}^{\Delta}$	0.99	**0.57**	0.21	0.18			
	48. Viverridae	34	30	18.1[26]	Supertree[26]	24.6	$\sqrt[3]{Mass}^{\Delta}$	0.56	**0.60**	0.17	0.23			
Amphibians	49. *Desmognathus*	23	23	20[28]	Bayes+PL[28]	38	SVL[28]	1.22	**0.56**	0.15	0.29			

*, new ML phylogeny prepared; **, mass of final instar; Δ, unpublished data; †, tarsus length also used; ‡, age based on molecular calibration from fossil data; ◊ includes *Dives*, *Euphagus*, *Quiscalus*, *Qgelaius*, *Molothrus*, and *Scaphidura*; § includes *Gnorimopsar*, *Oreopsar*, *Agelaioides*, *Chrysomus*, *Xanthospar*, *Pseudoleistes*, *Curaeus*, *Agelasticus*, *Lampropsar*, *Gymnomystax*, and *Macroagelaius*. References: [1]Shochat and Dessauer 1981; [2]Nicholson et al. 2005; [3]Harmon et al. 2003; [4]Townsend and Larson 2002; [5]Harmon et al. 2008; [6]Austin et al. 2004; [7]Jennings et al. 2003; [8]Torres-Carvajal et al. 2006; [9]Ast 2001; [10]Pepin 2001; [11]Petren et al. 2001; [12]Lack 1947; [13]Grant and Grant 2002; [14]Mooers et al. 1999; [15]Near et al. 2003; [16]Collar et al. 2005; [17]Near et al. 2005; [18]Joyce et al. 2005; [19]Page et al. 2003; [20]Near and Keck 2005; [21]Near and Benard 2004; [22]Turgeon et al. 2005; [23]Stoks et al. 2005; [24]Gillespie et al. 1994; [25]Gillespie 2004; [26]Bininda-Emonds et al. 2007; [27]Vos and Mooers 2006; [28]Kozak et al. 2005.

phylogenies onto chronograms from recent studies of tetrapod diversification (Vitt et al. 2003; Vos and Mooers 2006; Bininda-Emonds et al. 2007; Hugall et al. 2007).

Most phylogenies were constructed using maximum-likelihood or Bayesian analysis of molecular gene sequence data, although eight of the trees were derived from supertree analysis and two using Unweighted Pair Group Method with Arithmetic Mean (UPGMA; Table 1). We calculated branch lengths using fossil age calibrations and either a strict or relaxed molecular clock (Table 1). We also estimated the absolute age of the root node of each tree (i.e., the crown age of each clade) from literature or unpublished data (Table 1).

We compiled a variety of indices of body size for species in each clade from museum specimens or previous literature (Table 1). These data were converted to a linear scale where necessary (e.g., by taking the cube-root of mass) and log-transformed. Because we were interested in comparing net rates of body size evolution, we standardized these data by dividing by an estimate of the average within-species standard deviation in body size. We did not have enough samples within species to estimate this standard deviation from our data. Instead, we use an average value calculated across 210 taxonomically varied animal species (0.0772, McKellar and Hendry 2009).

For most clades (39 of 49), we also generated a body shape axis by performing a principal components analysis on the correlation matrix of a set of log-transformed measurements. In all of these datasets, PC1 provided an index of body size and was strongly positively correlated with all original character axes. We obtained an independent axis of body shape by retaining the second axis (PC2), or (when only two characters were measured) by obtaining the residuals from a regression of a log-transformed trait on the log-transformed body size measurement. Principal component loadings and the proportion of the total variance explained by PC2 are available in the Appendix (Table S1). Data are available on Dryad (http://www.datadryad.org/).

We compared fits of three different models to each dataset using the Akaike information criterion, corrected for sample size (AICc; Sugihara 1978): a random walk (BM, modeled as Brownian motion); a random walk with a single stationary peak (SSP), such that trait values have a tendency to return to a medial value (SSP, modeled as an Ornstein–Uhlenbeck process; Hansen 1997; Butler and King 2004); and an EB model in which the net rate of evolution slows exponentially through time as the radiation proceeds (EB, modeled as a BM process with a time-dependent dispersion parameter; Blomberg et al. 2003; Freckleton and Harvey 2006). We also compared the fit of the three models to various subtrees and supertrees constructed from our data (see Results).

Under each of the three models (BM, SSP, and EB), expected tip values follow a multivariate normal distribution with an expected mean vector $\mathbf{E}(\mathbf{X})$ and covariance matrix, $\mathbf{V}$ determined by the model and phylogenetic tree. Each set of tip values has a likelihood:

$$L = \frac{\exp\left\{-1/2[\mathbf{X} - \mathbf{E}(\mathbf{X})]'(\mathbf{V})^{-1}[\mathbf{X} - \mathbf{E}(\mathbf{X})]\right\}}{\sqrt{(2\pi)^N \cdot \det(\mathbf{V})}}, \quad (1)$$

where $\mathbf{X}$ is a vector of phenotypic values for the species in the tree, N is the number of species, and prime ($'$) denotes transpose. Under the BM model, there are two parameters. Expected tip values follow a multivariate normal distribution with an expected mean vector $\mathbf{E}(x) = \bar{z}_o$, a parameter representing the ancestral state value for the clade, and an expected covariance matrix $\mathbf{V}$, with elements $V_{ij} = \sigma^2 s_{ij}$, where s_{ij} are the elements of a matrix $\mathbf{S}$ representing the shared path length from the root to the common ancestor of taxa i and j and σ^2 is a parameter describing the rate at which taxa diverge from each other through time (Felsenstein 1973; see also Ackerly 2009). We refer to this parameter as an estimate of evolutionary "net rate," bearing in mind that the dispersion of phenotypes under a random-walk model is different from one in which traits change directionally through time (Bookstein 1987). For the SSP model, $\mathbf{V}$ is derived from the expectation under an Ornstein–Uhlenbeck model of evolution, and has elements (Hansen 1997; Butler and King 2004)

$$V_{ij} = \frac{\sigma^2}{2\alpha} e^{-2\alpha(T - s_{ij})}(1 - e^{-2\alpha s_{ij}}) \quad (2)$$

where σ^2 and α are the net rate and constraint parameters of the model, T is the time of the deepest split in the tree, and $\mathbf{S}$ is a matrix whose elements s_{ij} are described above. This model has four parameters: $\bar{z}_o$, the ancestral state; θ, the trait optimum; σ^2, the net rate parameter; and α, the strength of the constraint moving trait values back toward the optimum. However, when fitting an SSP model to comparative data with ultrametric trees, the maximum-likelihood ancestral state and trait optimum are equal, and the model reduces to three parameters. This model is equivalent to BM if $\alpha = 0$. Finally, under the EB model, $\mathbf{V}$ has elements (Blomberg et al. 2003)

$$V_{ij} = \int_0^{s_{ij}} \sigma_o^2 e^{rt}\, dt = \sigma_o^2 \left(\frac{e^{r s_{ij}} - 1}{r}\right). \quad (3)$$

This model has three parameters: $\bar{z}_o$, the estimated ancestral state for the clade; σ_o^2, the initial value for the net rate parameter; and r, a parameter describing the pattern of rate change through time. We restricted r to values below zero to correspond with a model in which net rates decrease through time; when $r = 0$, this model reduces to the BM model. Our statistical approach has sufficient power to distinguish among these three models for moderately sized phylogenetic trees, although for reasonable parameter values, power to detect the EB model is much lower than power to detect the SSP model (see Appendix).

All three models are compatible with a range of evolutionary processes. For example, BM can result from both genetic drift and directional selection where the direction of selection fluctuates randomly through time (Felsenstein, 1988). Similarly, evolution resembling an OU model on an SSP can be produced when both natural selection toward an optimum and random drift act on a phenotypic character (Lande 1976; Felsenstein 1988), or when neutral evolution takes place in a tightly constrained part of morphospace such that trait values are limited to a certain range. Because our implementation of the EB model is new, we will discuss it in more depth. This model is meant to be a general model of increasing constraints on evolutionary change through the course of an adaptive radiation, as would be produced by, for example, increasing interspecific competition as niches become filled. There are a number of ways one might model such a process. For example, one might impose a constraint parameter that becomes stronger through time, or one might allow deep clades in a phylogenetic tree to have separate optima, within which there are strong constraints. We focus on one simple implementation in which net rates of morphological change decline exponentially through time. We consider some alternatives in the Appendix. Any of these models would fit data that showed rates that slow through time, regardless of the form of that slowdown, better than the BM or SSP models.

Conceptually, the main difference between the SSP and EB models relates to the expected variance in trait values of young subclades within each higher clade. SSP predicts that young subclades will capture much of the variation in trait values and thus be approximately as variable as older, more inclusive groups, whereas EB predicts that young subclades, diversifying at the end of a presumed radiation, will exhibit less variation than older, more inclusive clades (Fig. 1; see also Harmon et al. 2003).

For all three tested models, we used a search algorithm to find maximum-likelihood parameter values for each clade. We then compared the overall fit of these three models to the entire body size and shape dataset by calculating the product of the likelihood of each model across all trees, and computed the Akaike weights for each. For a given phylogenetic tree size, one has less power to detect EB when it is the true model of evolution compared to SSP (see Appendix). We also computed model-averaged parameter estimates following Burnham and Anderson (1998).

Measurement error can cause a significant bias in evolutionary rate reconstructions, such that rates near the tips are overestimated (Martins 1994). To account for this effect, we modeled measurement error directly by adding variation to the diagonal of the expected among-species variance–covariance matrix (O'Meara et al. 2006). We present results based on a standard error equal to 0.0345 on a natural log scale, representing the expected error for sample size of five individuals per species given an average within-species standard deviation of 0.0772. We also analyzed the data assuming other levels of measurement error; these analyses did not qualitatively affect our results.

Results

Analysis of individual clades showed that the time course of morphological evolution differ substantially among clades. Maximum likelihood estimate of model parameter values and, for clades with at least 10 species, the Akaike weights for the BM, SSP, and EB models mostly supported a BM model (Tables 2 and 3; BM: body size, 25/38, body shape, 14/29), but a substantial number favored an SSP model (body size: 12/38; body shape, 14/29; Fig. 2; see also Appendix Tables 2 and 3). Only two datasets showed weak support for the EB model (Fig. 2, Table 3; maximum Akaike weight: body size, 0.63, *Varanus* lizards; body shape, 0.61, pygopodid lizards). Results were roughly similar across body size and shape, although body shape appears to be constrained more often than body size (Table 2). When we pooled the results for each model across datasets by multiplying the likelihoods across all trees, we found very strong support for the SSP model for

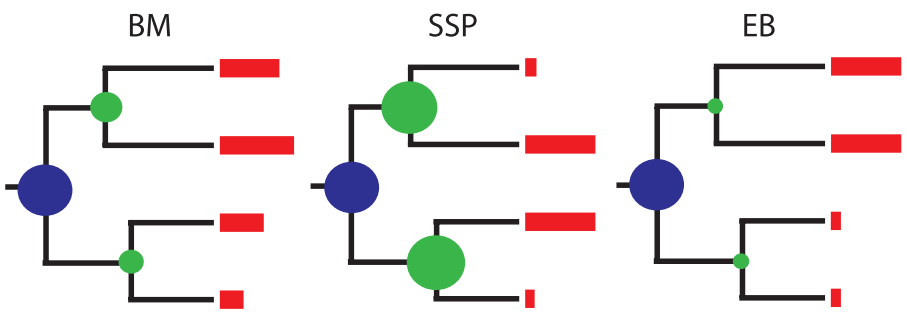

Figure 1. **Example illustrating the differing predictions for the BM (Brownian motion), SSP (single stationary peak), and EB (early burst) models of morphological evolution. A hypothetical phylogenetic tree of four species is depicted. The length of each red line at the tips of each tree indicates the magnitude of a given morphological character for each species. Green circles indicate the amount of variation within subclades in the tree, whereas blue circles indicate the amount of variation in the whole clade. Subclades have much lower variation under the EB model, and greater variation under the SSP model, when each is contrasted to the BM model.**

Table 2. Number of clades and subclades with $n>10$ species showing support for each of the three models (BM, SSP, and EB) for body size and body shape. We count both the number of clades with the highest AICc values for a particular model ("maximum w") and those with weights greater than 0.95 ("w>0.95").

Clades	Dataset	Number of phylogenies	Criterion	BM	SSP	EB
All full clades	Body size	49	Maximum w	25	12	1
			w>0.95	0	6	0
	Body shape	39	Maximum w	14	14	1
			w>0.95	0	8	0
All subclades	Body size	284	Maximum w	215	61	10
			w>0.95	0	21	0
	Body shape	205	Maximum w	103	99	5
			w>0.95	0	36	0

both body size and shape across almost all the major taxonomic groups (amphibian, bird, fish, insect, mammal, or squamate) in our dataset (Table 3).

Model-averaged parameter values varied widely across datasets but showed the same general pattern. In some cases, we could not estimate parameters for the SSP model because the likelihood surface exhibited a flat ridge (see Butler and King 2004). Excluding those datasets, we found a range of model-averaged estimates for the net rate parameter σ^2 (body size, expressed as the expected variance in trait means per million years in units of within-population standard deviations, 42 clades, mean $\sigma^2 = 0.74$, range: 0.00032–10.9; body shape net rate parameter estimates are unit dependent and cannot be compared; see Appendix) and the constraint parameter α (body size, 42 clades, mean $\alpha = 0.34$, range: 0–8.2; body shape, 33 clades, mean $\alpha = 1.55$, range: 0–20.5; see Appendix). Model-averaged estimates for r, the parameter from the EB model that describes the rate at which trait evolution slows through time, were generally very small (body size, 41 clades, mean $r = -0.0071$, range: -0.15 to 0; body shape, 35 clades, mean $r = -0.0036$, range: -0.041 to 0; see Appendix).

The lack of EB patterns might be due, in part, to our choice of focal clades. To address this problem, we considered both smaller subsets and larger combinations of our focal clades. When we fit models to all subclades within trees with 10 or more species from every tree (body size: 284 subclades, body shape 205 subclades, some overlapping), results were consistent; most clades favored BM (body size: 215/284, body shape: 103/205) or SSP (body size: 61/284, body shape: 99/205) over the EB model (body size: 10/284, body shape: 5/205), but when there was strong support for a single model (Akaike weight > 0.95), SSP was always favored (57 cases, Table 2). When we analyzed body size evolution

Table 3. Results of model fitting tests combining likelihoods across all clades (size: 49 phylogenies, n=1484; shape: 39 phylogenies, n=1094) and various taxonomic subsets. N_c gives the number of clades, and N_p the number of parameters, for each model. Higher lnL and lower ΔAIC values indicate better model support; the best-supported model is in bold.

			BM			SSP			EB		
Clades	Phenotype	N_c	N_p	lnL	ΔAIC_{BM}	N_p	lnL	ΔAIC_C	N_p	lnL	ΔAIC_{EB}
All	Body size	49	98	−3696.6	134.9	147	**−3580.2**	**0**	147	−3690.5	220.7
	Body shape	39	78	−853.6	132.0	117	**−748.6**	**0**	117	−851.1	205.1
Squamates	Body size	11	22	−1496.3	3.9	33	**−1483.3**	**0**	33	−1493.3	19.9
	Body shape	11	22	−174.5	54.5	33	**−136.2**	**0**	33	−172.5	72.5
Birds	Body size	21	42	**−438.4**	**0**	63	−421.0	7.2	63	−437.0	39.2
	Body shape	20	40	−369.4	44.8	60	**−327.0**	**0**	60	−369.0	84.1
Fish	Body size	6	12	−729.9	145.9	18	**−651.0**	**0**	18	−729.9	157.9
	Body shape	5	10	−280.5	13.2	15	**−268.9**	**0**	15	−280.5	23.2
Insects	Body size	3	6	−191.0	6.6	9	**−184.7**	**0**	9	−190.6	11.7
	Body shape	1	2	**−66.5**	**0**	3	−66.4	1.9	3	−66.5	2.0
Mammals	Body size	7	14	**−781.0**	**0**	21	−780.1	12.3	21	−780.4	12.8
	Body shape	2	4	39.6	23.6	6	**52.4**	**0**	6	27.6	27.6
Amphibians	Body size	1	2	**−60.0**	**0**	3	−60.0	2.0	3	−59.3	0.6

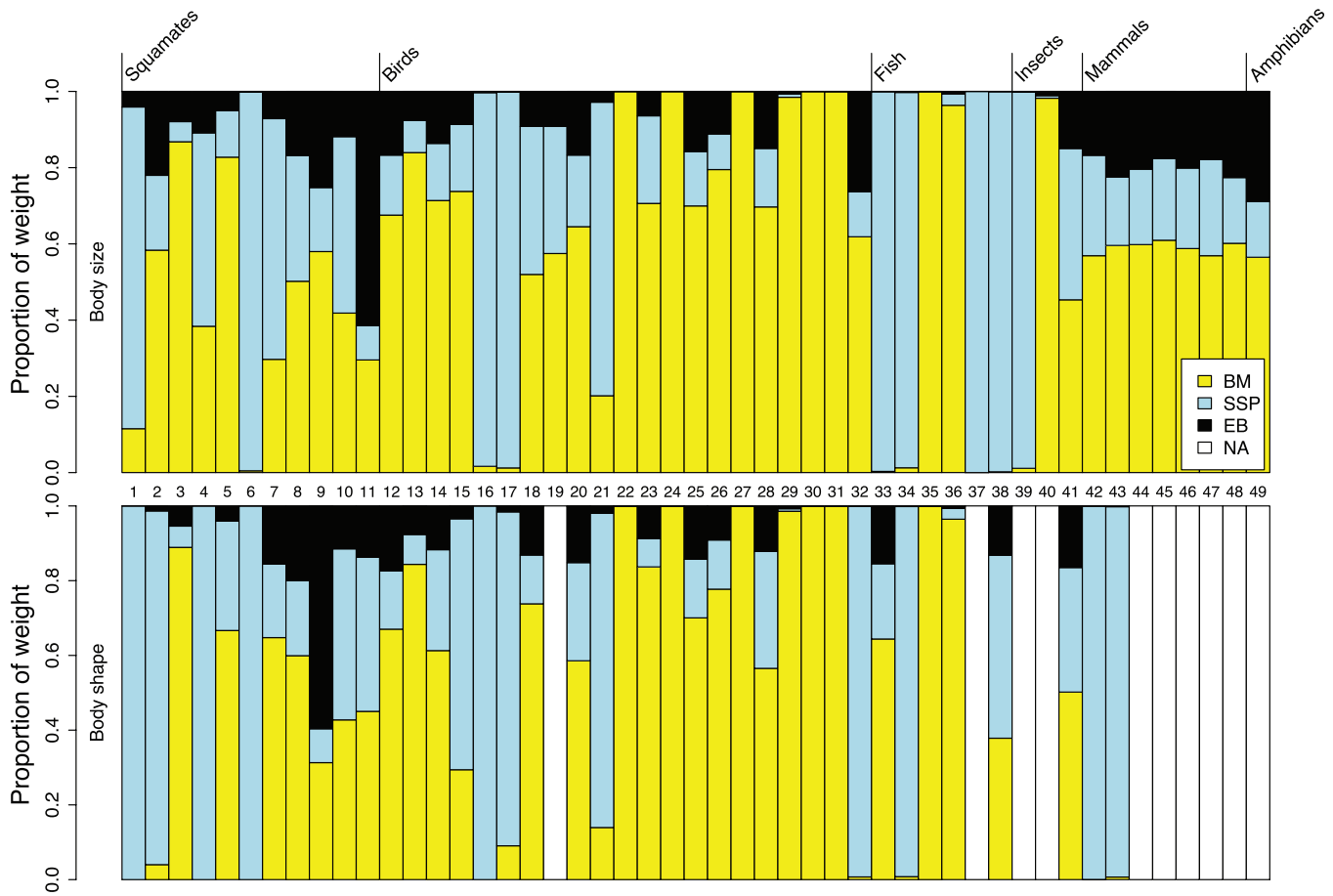

Figure 2. Akaike weights for three models of phenotypic evolution (BM, Brownian motion; SSP, single stationary peak; EB, early burst; NA, not applicable because shape data were unavailable) for all phylogenetic trees in the dataset. Numbers correspond to the datasets as listed in Table 1. Relative area of the bar filled with any color is proportional to the Akaike weight for that model given the data.

in combined trees made by pasting individual trees together by taxonomic group into larger "supertrees," only birds supported the EB model (Akaike weight = 0.98). Another of these large trees, carnivores, weakly supported the SSP model (Akaike weight = 0.66), whereas the other two major clades (squamates, primates) did not support any one model (all Akaike weights < 0.6; Table 4).

We have represented one particular pattern predicted to result from adaptive radiation with our EB model; however, the term adaptive radiation is sometimes used to describe evolution that occurs at a fast net rate, regardless of whether that rate slows through time. Indeed, estimated net rates of body size evolution of clades under a BM model spanned four orders of magnitude (Fig. 3; we limit our rate comparisons to body size because comparing net rates of body shape evolution across clades is problematic due to differing scales of measurement). Although some clades appeared to be evolving more quickly than others, the best predictor of net evolutionary rate is crown clade age (the age of the most recent common ancestor of all living species); the net rate of body size evolution was faster in the younger clades, with the oldest groups showing the slowest net rates of evolution ($r = -0.38$, $P < 0.01$ from simulations described in the Appendix; Fig. 3). Birds were the only group that did not show such a relationship. Body size in most bird clades evolved slowly compared with other clades of the same age (Fig. 3). Excluding birds from the analyses strengthened the negative relationship between net rate and age ($r = -0.80$, $P < 0.01$ from simulations described in the Appendix; Fig. 3). The slope of this relationship did not vary significantly within each group of nonbird higher taxa (amphibian, fish, insect, mammal, or squamate; see Appendix). Because our data mix several kinds of measurements and our analyses compare net rates across different time intervals, we carried out a series of analyses, summarized in the Appendix, which demonstrate that our patterns are robust and are not a statistical artifact of our methods.

Discussion

We find surprisingly little evidence for the EB model of morphological change in our comparative datasets. If EB-like patterns

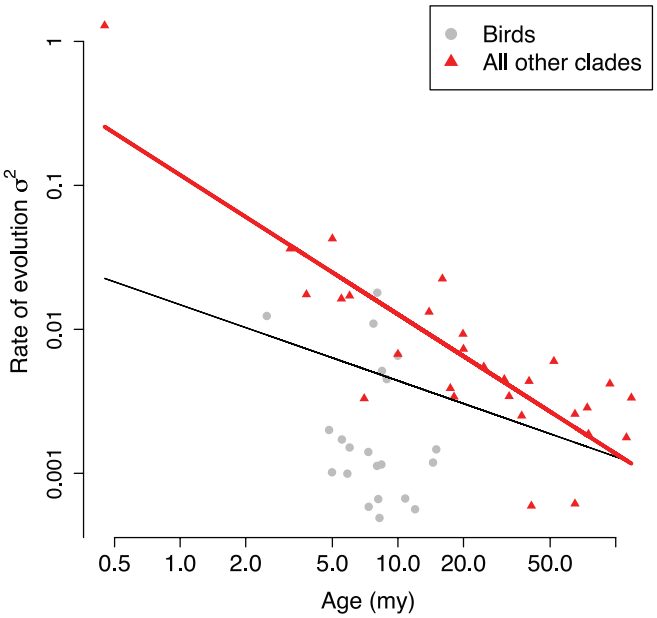

Figure 3. Relationship between clade age and average rate of body size evolution. Rates were calculated using maximum-likelihood under a Brownian motion model, and represent the expected variance in body size accumulated per million years. Gray circles represent bird clades, with all other clades as red triangles. Lines are least-squares regressions, with the thin black line including birds and the thick red line excluding them.

were common across the tree of life, one would expect to detect them in a dataset of this size even given the relatively low power of this test (see Appendix). Although our groups include many classic adaptive radiations, very few clades show patterns of rapid morphological evolution followed by relative stasis. Within classic adaptive radiations, it is often the case that young pairs of sister species are still morphologically very divergent, suggesting that the adaptive zone occupied by these species is not saturated. This suggests that radiations characterized by "EBs" of morphological evolution followed by slowdowns are rare. It is possible that this particular pattern is not a necessary part of adaptive radiation.

Our model-averaged value for the net rate of body size evolution is 0.74 phenotypic standard deviations per million years. The average generation time of our clades ranges from roughly five months to five years (mean = 20.5 months). Using this mean, we calculate an average net rate of $\sigma^2 \approx 1.2 \times 10^{-6}$ phenotypic standard deviations per generation (using the range of generation times, $\sigma^2 \approx 3.1 \times 10^{-7} - 3.7 \times 10^{-6}$).

Under a purely neutral model of genetic drift, phenotypes evolve according to a BM model with per-generation variance $\sigma^2 \approx h^2/N_e$ where h^2 is trait heritability and N_e effective population size (Lande 1976). Assuming that heritability for body size across these species is 0.4 (a typical value for morphological characters, Estes and Arnold 2007), this net rate is compatible only with very large N_e (~300,000), much higher than the typical range for species in the wild (~10–100,000; Estes and Arnold 2007). In other words, traits seem to be evolving too slowly to be explained by a purely neutral model of genetic drift.

When any of our datasets strongly supported a single model, it was typically a model of strong constraints. Lande (1976) described a model in which a population evolves on a constant adaptive peak and, over time, phenotypic evolution follows the pattern described by our SSP model. Model-averaged parameter estimates for our SSP model can thus be compared to empirical estimates of population size, heritability, and the strength of stabilizing selection in Lande's (1976) model. Under this model, $\sigma^2 = h^2/N_e$ and $\alpha = \omega^2/2N_e$ (Lande 1976) where ω^2 is the strength of stabilizing selection. These two parameters describe the net rates of evolution over short (σ^2) and long (α) time scales (Hansen 1996; Hansen and Martins 1996). Typical values of ω^2 in the wild range from 3 to 50 with a mode of around 3 (Estes and Arnold 2007), and so one would need either very small effective population sizes (<10) or extremely strong stabilizing selection, or both, to correspond with the relatively large values of α estimated for our comparative data (see Appendix). Thus, under the SSP model, we find that net rates of phenotypic change are too fast over short time scales (high estimated σ^2) but too slow over long time scales (large estimated α) to be explained by long-term

Table 4. Results of model fitting tests within various combined supertrees. Higher AIC weights indicate better support of the model from our data.

Model		BM		SSP			EB		
Phylogenetic tree	*n*	σ^2	Akaike weight	σ^2	α	Akaike weight	σ^2	*r*	Akaike weight
Birds	236	0.92	0.012	0.92	0.001	0.004	74.6	−0.05	0.98
Squamates	554	0.54	0.32	0.59	0.003	0.57	0.54	0	0.12
Mammals	325	1.20	0.45	1.31	0.009	0.38	1.20	0	0.16
Carnivores	192	1.53	0.25	1.93	0.03	0.66	1.53	0	0.09
Primates	133	0.71	0.59	0.71	0	0.21	0.71	0	0.21

stabilizing selection of the magnitude typically estimated in field studies.

Thus, although we find support for constrained models of evolution, models invoking stabilizing selection around a single stationary peak require very weak selection, unrealistically small population sizes, or both. Our broad-scale comparative dataset shows clearly that additional mechanisms are required to explain patterns of long-term stasis (Hansen 1997). For example, oscillating selection might be common in natural populations, such that rapid evolution over short time scales is often counteracted by reversals (Gibbs and Grant 1987; Siepielski et al. 2009). Alternatively, developmental biology and genetics have revealed multiple instances of constraints directing evolutionary change (Barton and Partridge 2000; Gould 2002). Another possible mechanism involves the interaction between natural selection and the complex geographic structure of species: new trait values can evolve quickly within local populations, but stabilizing selection over a species' entire range appears to strongly constrain long-term evolutionary trajectories (Eldredge et al. 2005). Although our SSP model should capture some of the dynamics of these nonstabilizing selection constraints, the parameter estimates of the SSP model do not seem to match what is known about actual microevolutionary processes. Future work requires the application of more complex models, such as the peak-shift models described in Estes and Arnold (2007), to interspecific comparative data.

Despite the overall support for constrained models, the dynamics of trait evolution varied substantially among clades (Figs. 2 and 3). Future work could investigate differences among taxa or traits in the tempo and mode of evolution. For example, one large clade (all birds) strongly supported the EB model and showed patterns of body size evolution consistent with adaptive radiation (see also Starck and Ricklefs 1998). Another recent study showed a clear pattern of decreasing rates of change through time of skeletal characters in early tetrapod evolution (Ruta et al. 2006). It is possible that evolution involves long periods of constraint punctuated by brief periods of directional selection (Gould 2002; Butler and King 2004; Estes and Arnold 2007); our results suggest, however, that such periods may be quite rare. Fitting models that include explicit dynamics of populations evolving on adaptive landscapes might help to resolve this issue (Estes and Arnold 2007). Additionally, the amount of range overlap among species likely influences diversification, such that groups with a larger proportion of sympatric species early in their history might more likely exhibit an EB pattern of adaptive radiation as species interact and coevolve while filling ecological space (Schluter 2000; Harmon et al. 2003).

Our finding of high net rates of evolution over short time scales agrees with previous results from a wide range of data sources (Stanley 1975; Gingerich 1983, 2001; Lynch 1990; Hendry and Kinnison 1999; Kinnison and Hendry 2001; Roopnarine 2003; Estes and Arnold 2007), and is consistent with the support in many of our clades for the SSP model; rapid change is only apparent in young clades, but the pattern is obscured by constraints on evolution over long time scales. This is because our estimates of net rate effectively divide the amount of change by the time interval for that change. Under the SSP model, the effects of constraints on the overall amount of change are most apparent over long time periods. Because of this, species in older clades show similar amounts of change as species in younger clades, but over a longer time interval, and thus have lower apparent net rates of evolution.

In this study, we considered only the evolutionary divergence of extant taxa based on their phylogenetic relationships, rather than direct historical information from fossils. Fossils can provide estimates of evolutionary rates (Gingerich 1983, 2001; Foote 1994), and similar model-fitting approaches can be used for fossil data (e.g., Hunt 2006). However, fossils are rare or absent from many clades suspected of recent adaptive radiation, such as Caribbean anoles, Galápagos finches, and East African cichlids. An approach that combines direct historical information from fossils with phylogenetic information could increase statistical power, and might reveal more details about the dynamics of trait evolution in these clades (Polly 2001; Hunt 2006; Ruta et al. 2006). In our analyses, we also ignored phylogenetic uncertainty in calculating evolutionary rates (O'Meara et al. 2006), a factor that could be incorporated into future work.

Our results suggest that a model of constant-rate BM, assumed by most comparative methods, fits some clades poorly. Instead, constraints on phenotypic evolution provide a potentially unifying explanation for the patterns we observed, and can explain the common observation of rapid evolution over short time scales and slower change over geological time scales (Eldridge et al. 2005; Estes and Arnold 2007).

For the traits and phylogenetic trees considered here, the model of adaptive radiation as a transient burst of morphological evolution at the base of a clade followed by stasis is rare. This could be because we have a nonrandom sample of trees, because "EBs" do not leave a long-term signal in patterns of trait distributions across extant species, or perhaps because such "EBs" are genuinely uncommon across the tree of life. This pattern stands in contrast to recent results suggesting that slowdowns in lineage diversification through time are common in comparative data (McPeek 2008; Phillimore and Price 2008; Rabosky and Lovette 2008). This contrast between patterns of lineage diversification and the accumulation of morphological disparity through time is worthy of future research. Despite these caveats, our results suggest the provocative conclusion that EBs followed by slowdowns are genuinely uncommon across a broad portion of the tree of life, even among clades that represent some of the most cherished examples of adaptive radiations.

ACKNOWLEDGMENTS

We wish to thank A. Larson, J. Alroy, and P. Wagner for insightful discussions. M. Alfaro, T. Hagey, D. Jochimsen, N. Reid, E. B. Rosenblum, S. J. Arnold, J. Uyeda, and four anonymous reviewers provided helpful comments. This work was conducted as a part of the Adaptive Radiations Working Group supported by the National Center for Ecological Analysis and Synthesis, a Center funded by NSF (EF-0553768), the University of California, Santa Barbara, and the State of California. BLS was supported by a postdoctoral fellowship from the National Evolutionary Synthesis Center, NESCent (NSF EF-0423641). AOM is supported by an NSERC Discovery Grant.

LITERATURE CITED

Ackerly, D. 2009. Conservatism and diversification of plant functional traits: evolutionary rates versus phylogenetic signal. Proc. Natl. Acad. Sci. USA 106:19699–19706.

Ast, J. C. 2001. Mitochondrial DNA evidence and evolution in Varanoidea (Squamata). Cladistics 17:211–226.

Austin, J. J., E. N. Arnold, and C. G. Jones. 2004. Reconstructing an island radiation using ancient and recent DNA: the extinct and living day geckos (*Phelsuma*) of the Mascarene Islands. Mol. Phylogenet. Evol. 31:109–122.

Baldwin, B. G., and M. J. Sanderson. 1998. Age and rate of diversification of the Hawaiian silversword alliance (Compositae). Proc. Natl. Acad. Sci. USA 95:9402–9406.

Barton, N., and L. Partridge. 2000. Limits to natural selection. BioEssays 22:1075–1084.

Bininda-Emonds, O. R. P., M. Cardillo, K. E. Jones, R. D. E. MacPhee, R. M. D. Beck, R. Grenyer, S. A. Price, R. A. Vos, J. L. Gittleman, and A. Purvis. 2007. The delayed rise of present-day mammals. Nature 446:507–512.

Blomberg, S. P., T. Garland, and A. R. Ives. 2003. Testing for phylogenetic signal in comparative data: behavioral traits are more labile. Evolution 57:717–745.

Bookstein, F. L. 1987. Random walk and the existence of evolutionary rates. Paleobiology 13:446–464.

Butler, M. A., and A. A. King. 2004. Phylogenetic comparative analysis: a modeling approach for adaptive evolution. Am. Nat. 164:683–695.

Collar, D. C., T. J. Near, and P. C. Wainwright. 2005. Comparative analysis of morphological diversity: does disparity accumulate at the same rate in two lineages of centrarchid fishes? Evolution 59:1783–1794.

Eldredge, N., J. N. Thompson, P. M. Brakefield, S. Gavtilets, D. Jablonski, J. B. C. Jackson, R. E. Lenski, B. S. Lieberman, M. A. McPeek, and W. Miller III. 2005. The dynamics of evolutionary stasis. Paleobiology 31:133–145.

Endler, J. A. 1986. Natural selection in the wild. Princeton Univ. Press, Princeton, NJ, 354 pp.

Estes S., and S. J. Arnold. 2007. Resolving the paradox of stasis: models with stabilizing selection explain evolutionary divergence on all timescales. Am. Nat. 169:227–244.

Felsenstein, J. 1973. Maximum-likelihood estimation of evolutionary trees from continuous characters. Am. J. Hum. Genet. 25:471–492.

———. 1988. Phylogenies and quantitative characters. Ann. Rev. Ecol. Syst. 19:445–471.

Fisher, R. A. 1930. The genetical theory of natural selection. Clarendon Press, Oxford, 318 pp.

Foote, M. 1994. Morphological disparity in Ordovician-Devonian crinoids and the early saturation of morphological space. Paleobiology 20:320–344.

Freckleton, R. P., and P. H. Harvey. 2006. Detecting non-Brownian trait evolution in adaptive radiations. PLoS Biol. 4:e373.

Gibbs, H. L., and P. R. Grant. 1987. Oscillating selection on Darwin's finches. Nature 327:511–513.

Gillespie, R. G. 2004. Community assembly through adaptive radiation in Hawaiian spiders. Science 303:356–359.

Gillespie, R. G., H. B. Croom, and S. R. Palumbi. 1994. Multiple origins of a spider radiation in Hawaii. Proc. Natl. Acad. Sci. USA 91:2290–2294.

Gingerich, P. D. 1983. Rates of evolution: effects of time and temporal scaling. Science 222:159–161.

———. 2001. Rates of evolution on the time scale of the evolutionary process. Genetica 112–113:127–144.

Givnish, T. J. 1997. Adaptive radiation and molecular systematics: issues and approaches. Pp. 1–54 *in* T. J. Givnish and K. J. Sytsma, eds. Molecular evolution and adaptive radiation. Cambridge Univ. Press, Cambridge.

Givnish, T. J. 1999. Adaptive radiation, dispersal, and diversification of the Hawaiian lobeliads. Pp. 67–90 *in* M. Kato, ed. The biology of biodiversity. Springer-Verlag, Tokyo.

Givnish, T. J., and K. J. Systma, eds. 1997. Molecular evolution and adaptive radiation. Cambridge Univ. Press, Cambridge, 640 pp.

Gould, S. J. 2002. The structure of evolutionary theory. Harvard Univ. Press, Cambridge, 1464 pp.

Grant, P. R., and B. R. Grant. 2002. Unpredictable evolution in a 30-year study of Darwin's finches. Science 296:707–711.

———. 2008. How and why species multiply: the radiation of Darwin's finches. Princeton Univ. Press, Princeton, NJ, 272 pp.

Hansen, T. F. 1997. Stabilizing selection and the comparative analysis of adaptation. Evolution 51:1341–1351.

Hansen, T. F., and E. P. Martins. 1996. Translating between microevolutionary process and macroevolutionary patterns: the correlation structure of interspecific data. Evolution 50:1404–1417.

Harmon, L. J., J. A. Schulte II, A. Larson, and J. B. Losos 2003. Tempo and mode of evolutionary radiation in Iguanian lizards. Science 301:961–964.

Harmon, L. J., J. Melville, A. Larson, and J. B. Losos. 2008. The role of geography and ecological opportunity in the diversification of day geckos (Phelsuma). Syst. Biol. 57:562–573.

Hendry, A. P., and M. T. Kinnison. 1999. The pace of modern life: measuring rates of contemporary microevolution. Evolution 53:1637–1653.

Hunt, G. 2006. Fitting and comparing models of phyletic evolution: random walks and beyond. Paleobiology 32:578–601.

Jennings, W. B., E. R. Pianka, and S. Donnellan. 2003. Systematics of the lizard family Pygopodidae with implications for the diversification of Australian temperate biotas. Syst. Biol. 52:757–780.

Joyce, D. A., D. H. Lunt, R. Bills, G. F. Turner, C. Katongo, N. Duftner, C. Sturmbauer, and O. Seehausen. 2005. An extant cichlid fish radiation emerged in an extinct Pleistocene lake. Nature 435:288–298.

Kinnison, M. T., and A. P. Hendry. 2001. The pace of modern life II: from rates of contemporary microevolution to pattern and process. Genetica 112–113:145–164.

Kozak, K. H., A. Larson, R. M. Bonett, and L. J. Harmon. 2005. Phylogenetic analysis of ecomorphological divergence, community structure, and diversification rates in dusky salamanders (plethodontidae: *Desmognathus*). Evolution 59:2000–2016.

Lack, D. 1947. Darwin's Finches. Cambridge Univ. Press, New York, NY.

Lande, R. 1976. Natural selection and random genetic drift in phenotypic evolution. Evolution 30:314–334.

Linder, H. P. 2009. Plant species radiations: where, when, why? Philos. Trans. R. Soc. Lond. B 363:3092–3105.

Losos, J. B. 2009. Lizards in an evolutionary tree: ecology and adaptive radiation of anoles. Univ. of California Press, Berkeley, CA. 512 pp.

Losos, J. B., and D. B. Miles. 2002. Testing the hypothesis that a clade has adaptively radiated: iguanid lizard clades as a case study. Am. Nat. 160:147–157.

Lynch, M. 1990. The rate of morphological evolution in mammals from the standpoint of the neutral expectation. Am. Nat. 136:727–741.

Martins, E. P. 1994. Estimating the rate of phenotypic evolution from comparative data. Am. Nat. 144:193–209.

McKellar, A. E., and A. P. Hendry. 2009. How humans differ from other animals in their levels of morphological variation. PLoS ONE 4:e6876.

McPeek, M. A. 2008. The ecological dynamics of clade diversification and community assembly. Am. Nat. 172:E270–E284.

Mooers, A. Ø., S. M. Vamosi, and D. Schluter. 1999. Using phylogenies to test macroevolutionary hypotheses of trait evolution in cranes (Gruinae). Am. Nat. 154:249–259.

Near, T. J., and M. F. Benard. 2004. Rapid allopatric speciation in logperch darters (percidae: Percina). Evolution 58:2798–2808.

Near, T. J., and B. P. Keck. 2005. Dispersal, vicariance, and timing of diversification in Nothonotus darters. Mol. Ecol. 14:3485–3496.

Near, T. J., T. W. Kassler, J. B. Koppelman, C. B. Dillman, and D. P. Philipp. 2003. Speciation in North American black basses, Micropterus (Actinopterygii: Centrarchidae). Evolution 57:1610–1621.

Near, T. J., D. I. Bolnick, and P. C. Wainwright. 2005. Fossil calibrations and molecular divergence time estimates in centrarchid fishes (teleostei: Centrarchidae). Evolution 59:1768–1782.

Nee, S., A. O. Mooers, and P. H. Harvey. 1992. Tempo and mode of evolution revealed by molecular phylogenies. Proc. Natl. Acad. Sci. USA 89:8322–8326.

Nicholson, K. E., R. E. Glor, J. J. Kolbe, A. Larson, S. B. Hedges, and J. B. Losos. 2005. Mainland colonization by island lizards. J. Biogeogr. 32:929–938.

O'Meara, B. C., C. M. Ané, M. J. Sanderson, and P. C. Wainwright. 2006. Testing for different rates of continuous trait evolution using likelihood. Evolution 60:922–933.

Osborn, H. F. 1902. The law of adaptive radiation. Am. Nat. 36:353–363.

Page, M. L., M. Hardman, and T. J. Near. 2003. Phylogenetic relationships of barcheek darters (Percidae: *Etheostoma*, subgenus *Catonotus*) with descriptions of two new species. Copeia 2003:512–530.

Pepin, D. J. 2001. Natural history of monitor lizards (family Varanidae) with evidence from phylogeny, ecology, life history and morphology. PhD thesis, Washington Univ., St. Louis.

Petren, K., B. R. Grant, and P. R. Grant. 1999. A phylogeny of Darwin's finches based on microsatellite DNA length variation. Proc. R. Soc. Lond. B 266:321–329.

Phillimore, A. B., and T. D. Price. 2008. Density dependent cladogenesis in birds. PLoS Biol. 6:e71.

Polly, P. D. 2001. Paleontology and the comparative method: ancestral node reconstructions versus observed node values. Am. Nat. 157:596–609.

Rabosky, D. L., and I. J. Lovette. 2008. Density dependent diversification in North American wood-warblers. Proc. R. Soc. Lond. B. 275:2363–2371.

Roopnarine, P. D. 2003. Analysis of rates of morphological evolution. Ann. Rev. Ecol. Evol. Syst. 34:605–632.

Ruta, M., P. J. Wagner, and M. I. Coates. 2006. Evolutionary patterns in early tetrapods. I. Rapid initial diversification followed by decrease in rates of character change. Proc. R. Soc. Lond. B 273:2107–2111.

Schluter, D. 2000. The ecology of adaptive radiation. Oxford Univ. Press, Oxford. 296 pp.

Seehausen, O. 2006. African cichlid fish: a model system in adaptive radiation research. Proc. R. Soc. Lond. B 273:1–12.

Shochat, D., and H. C. Dessauer. 1981. Comparative immunological study of albumins of Anolis lizards of the Caribbean islands. Comp. Biochem. Physiol. 68A:67–73.

Siepielski, A. M., J. D. DiBattista, and S. M. Carlson. 2009. It's about time: the temporal dynamics of phenotypic selection in the wild. Ecol. Lett. 12:1261–1276.

Simpson, G. G. 1944. Tempo and mode in evolution. Columbia Univ. Press, New York. 237 pp.

———. 1953. The major features of evolution. Columbia Univ. Press, New York. 434 pp.

Stanley, S. M. 1979. Macroevolution: pattern and process. W. H. Freeman and Co, San Francisco, CA. 370 pp.

Starck, J. M., and R. E. Ricklefs. 1998. Variation, constraint, and phylogeny: comparative analysis of variation in growth. Pp. 247–265 *in* J. M. Starck and R. E. Ricklefs, eds. Avian growth and development: evolution within the Altricial-Precocial spectrum. Oxford Univ. Press, Oxford.

Stoks, R., J. L. Nystrom, M. L. May, and M. A. McPeek. 2005. Parallel evolution in ecological and reproductive traits to produce cryptic damselfly species across the Holarctic. Evolution 59:1976–1988.

Sugihara, N. 1978. Further analysis of the data by Akaike's information criterion and the finite corrections. Comm. Stat. Theory Methods A7: 13–26.

Torres-Carvajal, O., J. A. Schulte, and J. E. Cadle. 2006. Phylogenetic relationships of South American lizards of the genus Stenocercus (Squamata: Iguania): a new approach using a general mixture model for gene sequence data. Mol. Phylogenet. Evol. 39:171–185.

Townsend, T., and A. Larson. 2002. Molecular phylogenetics and mitochondrial genomic evolution in the Chamaeleonidae (Reptilia, Squamata). Mol. Phylogenet. Evol. 23:22–36.

Turgeon, J., R. Stocks, R. A. Thum, J. M. Brown, and M. A. McPeek. 2005. Simultaneous quaternary radiations of three damselfly clades across the Holarctic. Am. Nat. 165:E78–E107.

Vos, R. A., and A. Ø. Mooers. 2006. Inferring large phylogenies: the big tree problem. PhD thesis, Simon Fraser Univ., Vancouver, Canada.

Associate Editor: D. Posada

Supporting Information

The following supporting information is available for this article:

Appendix includes additional results and analyses.

Supporting Information may be found in the online version of this article.

Please note: Wiley-Blackwell is not responsible for the content or functionality of any supporting information supplied by the authors. Any queries (other than missing material) should be directed to the corresponding author for the article.